2005-01-2342

NVH optimization of truck cab floor panel embossing pattern

C.R. Fredö
Ingemansson Technology AB, Box 276, SE-401 24 Göteborg, Sweden

Anders Hedlund
Volvo 3 P - Product Development, Dept. 26552, VLU3, SE-405 08 Göteborg, Sweden

ABSTRACT

Improved sound comfort is a part of Volvo's continued development for improved driver environment. As a part of work in this area, a method for panel embossing optimization with respect to NVH is outlined and exemplified for a truck cab floor. The selection of shapes that build up the end-form is made such that the embossing pattern is guaranteed not to generate hidden corners that cause production problems.

Initial tests on a simply supported plate show that the natural frequency of the fundamental mode can be increased about ten times. The example shows a cab floor for which the process was used to minimize sound transmission. The optimization process was shown to be able to generate plate segments that were stiffer than the main beam structure. In other words, the main beam structure was found to limit how stiff the plates could be made while maintaining an acceptable end result for the NVH analysis.

The results show that the optimization enable noise transmission peaks to be shifted into acceptable RPM ranges (of short duration) and that the noise transmission is significantly reduced at idle and for most of the common RPM range. The optimized floor weight will be reduced compared to the reference floor since the optimized embossing pattern replaces the reinforcing cross beams. A remaining unwanted peak within the common RPM range is difficult to remove with embossing as it is affected by an acoustic cab resonance that is best counteracted through acoustic means.

INTRODUCTION

Improved sound comfort is a part of Volvo's continued development for improved driver environment. As a part of work in this area, a method for panel embossing optimization with respect to NVH is outlined and exemplified for a truck cab floor.

The selection of shapes that build up the end-form is made such that the embossing pattern is guaranteed not to generate hidden corners that cause production problems. The shapes tend to create also embossing patterns that are agreeable from an aesthetic point of view. In other words, the embossing shape optimization procedure can be used for visible surfaces.

A MOTIVATION TO THE SELECTION AND HANDLING OF EMBOSSING PATTERNS

It is well known that curvature affects the bending stiffness of a plate. However, how to vary curvature such that multi-disciplinary optimization goals can be reached necessitates the use of more than a single variable for curvature.

The embossing pattern selection is inspired by the findings of Rebillard and Guyader [1,2] on so called hypersensitivity where it was discovered that small changes in angle between two free-free flat plates made from aluminum or steel cause large shift in the dynamic response when plate angles vary between 2 and 5 degrees. Similar changes in angle have less of an impact for angles smaller than 2 degrees and for angles larger than 5 degrees.

The second insight is based on unpublished work by J. Plunt in which it was shown that variation in stiffness affect structure modes at which the correlation length coincides. In other words, long wavelength stiffness variation has a greater effect on low frequency modes than on high frequency modes and vice versa. The strongest effect is found when the stiffness distribution pattern coincides with the mode shape, i.e. when the correlation lengths of the mode shape and the stiffness variation match.

Extending the insights on correlation lengths leads to the hypothesis that the optimal embossing pattern for a particular mode shape is the mode shape itself. Stiffness variation is created by mode shape curvature. The insights on hyper sensitivity leads to the insight that the embossing depth governs the angle and that there should be an optimal stiffening interval.

In theory, one should work with all mode shapes as embossing shape functions. However, this does easily lead to optimization schemes that exceed most computational resources. Therefore, a more pragmatic approach was used in the current investigation. A noise transmission analysis was first made to identify the frequency at which the most noise is transmitted into the cab and related mode shapes. The mode shapes of the most 'noisy' modes were selected as the embossing shapes as these modes were of the largest importance to modify. Note that the selection of shapes can be based on criteria other than noise.

The absolute values of the mode shape is used in the generation of the final embossing pattern as this guarantees an end shape without hidden corners, i.e.

$$[\Phi]_{total} = C_1 \cdot |[\Phi_1]| + C_2 \cdot |[\Phi_2]| + ...C_n \cdot |[\Phi_n]| + , \qquad (1)$$

where the total embossing pattern is Φ_{total}, the embossing amplitude is C_n, the mode shape is Φ_n for mode n and the absolute value is signified as / /, Figure 1.

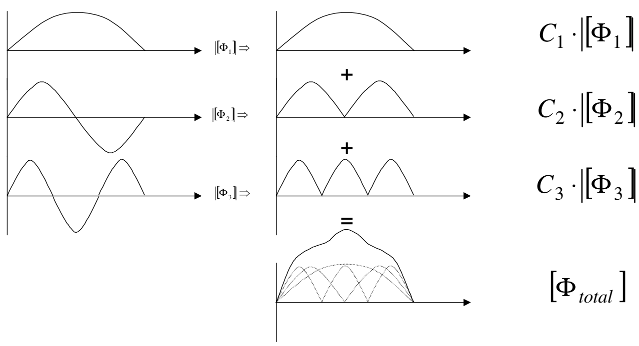

Figure 1. Workflow for the embossing pattern calculation. The absolute value of each mode is calculated and multiplied by an embossing amplitude factor before being summed into the final embossing pattern that is to be imprinted on the mesh. The example uses three mode shapes and three embossing amplitudes.

Requirements

The engine is the dominant source for cab noise. The operation pattern is well known for the engine and its orders generate the frequencies

$$f_{order} = N_{order} \cdot \frac{RPM}{60} , \qquad (3)$$

where *RPM* is the number of revolutions per minute, and N_{order} is the order number. For a straight 6-cylinder engine: uneven combustion is order 0.5, unbalance is order 1.0, the fundamental firing frequency is order 3.0 (the harmonics are 3.0, 6.0, 9.0 etc), camshaft operation is order 6.0 (harmonics at 12.0, 18.0 etc.).

Order 4.5 can excite a torsion mode in the powertrain at high RPM. The frequency range at which the torque excitation is significant falls into a 'well excited' zone of the 6[th] order, so the effects of this order is not included in the OK/NOT OK bar even though the order is included in the plot. The OK zones are defined as frequency ranges at which energy orders are expected to excite only during short time intervals and vice versa for the NOT OK zones.

Figure 2 shows that there are two frequency zones within which it is favorable to locate 'noisy modes'. The first zone is 35 Hz to 55 Hz and the second zone is 90 Hz to 120 Hz. Thus, these zones define the targets for the optimization. It should be observed that the definition of these frequency ranges can be ruined in the case that auxiliary equipment is given orders that produce frequencies that fall into these ranges and strongly excite the cab floor.

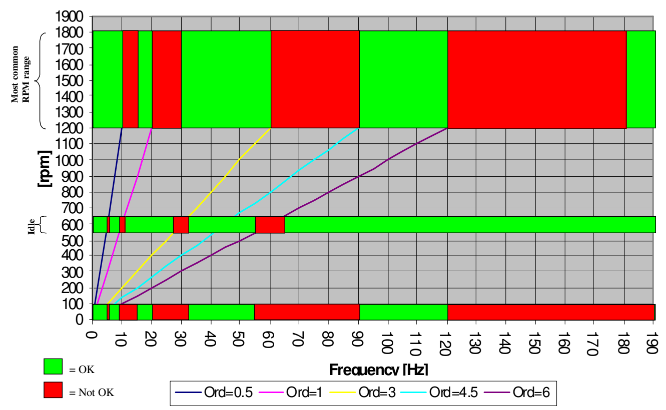

Figure 2. Frequencies generated by the engine orders and the most common engine operating speeds is used to define frequency intervals at which natural frequencies with high sound transmission/radiation. Some frequency bands are marked as (green) OK since they will not be excited by engine orders at normal driving conditions, e.g. the bands [35,55] Hz and [90,120] Hz. Therefore, it is OK to locate a noisy mode in a frequency range at which engine orders are expected only with short duration.

A MOTIVATION INTO THE TECHNICAL APPROACH

Figure 3 shows the flat cab floor that was used as the start out model and the floor coupled with the cab cavity. The cab floor is coupled to the cavity and the exterior domain using a SYSNOISE fully coupled BE analysis. Note that only the lower part of the floor is coupled to the cavity and that it is only this part of the floor structure that radiates to the exterior domain. Panels other than the cab floor panel are treated as rigid in the acoustic part of the model.

Noise Transfer Functions (NTFs), i.e. Pa/N, and Acoustic Transfer Functions (ATFs), i.e. $Pa/m^3/s^2$, are computed using reciprocity. Therefore, a volume velocity source is located at the driver's head centre and the acoustic pressure below the floor and the vibration at the support points for the cab structure are computed in the analysis. This is the most effective approach to the computation of this data.

The sound transmission analysis of the flat cab floor was used to identify the most 'noisy' modes. However, it is well known that modes with an odd number of half wavelengths transmit and radiate the most noise for plate structures in the frequency range considered, i.e. at frequencies below the coincidence frequency limit. As expected, the sound transmission analysis confirmed that the 'noisy' flat floor modes indeed were the 'odd' modes, Figure 7. The cab floor consists from three plate segments that are surrounded by beam structures. A total of six 'noisy' modes were thus selected to act as embossing shape functions.

A fully coupled sound transmission analysis requires about one hour computation, which turns optimization into a slow process should such analysis be made for each case in the optimization. A faster (approximate) scheme would be to compute uncoupled Acoustic Transfer Vectors that relate floor vibration to sound pressure e.g. at the driver and passenger head positions can be used to reduce simulation to the order of minutes. Floor vibration can then be caused by force- (structure) excitation as well as by pressure- (acoustic) excitation. However, such ATV software was not available to the end customer. A simpler scheme was therefore applied.

As mentioned above, modes with an odd number of half wavelengths are the noisy modes until the floor panels become so stiff that such 'generic' plate mode shapes cease to exist. It is the author's experience that such high degree of stiffening is not achieved until a fair amount of design iterations have been completed. Therefore, the simpler scheme was to project embossed cab floor modes shapes onto a selected set of predefined positions from which the number of half wavelengths per plate segment [N_x;N_y] can be extracted, Figure 4.

This simple approach may at first appear to be limited. However, modes that transmit noise effectively do also radiate noise effectively and the fact that pressure is not actually computed does not matter at early design stage. It is true that the simple scheme does not discriminate between structure and acoustic excitation, nor does it rate the response between modes. Reliable data that rank between acoustic and structure-borne sources or between directions and locations was not available to the project. Therefore, a more rigorous scheme can not be stated to be more valid than the simpler scheme applied herein before such data is available. The approach herein can be seen as a first stab at cab structure improvement that can be applied at early design phase.

Figure 2 shows the frequency bands at which noise transmission/radiation from engine order excitation is expected to be more acceptable. As above mentioned, the frequency bands 35-55 Hz and 90 – 120 Hz are used as targets for the natural frequencies of the noisy cab floor modes.

A Design of Experiments (DOE) plan was used to investigate the effect from embossing pattern on sound transmission, sound radiation into the cab and, implicitly also on structure-borne sound input. The embossing amplitude of the 'noisy' flat floor mode shapes are used as input variables. The output variables are the total embossing pattern depth, the natural frequencies of the 'noisy' modes and the total number of cab floor modes below 300 Hz.

Structure-borne power input is proportional to the modal density for force source excitation, i.e. the lesser the total number of modes up to a limiting frequency, the lesser the power input. Cab floor structure-borne excitation is input via the vibration isolators, i.e. excitation can be idealized as force source excitation whenever the isolation is functional. The structure-borne power input is

$$P_{in} = \frac{\pi \cdot n(\omega) \cdot |F|^2}{4 \cdot S \cdot m}, \quad (2)$$

where the modal density $n(\omega)$ is a function of angular frequency and is defined by the average separation in natural frequency in a band, the dynamic force amplitude is $|F|$, the plate surface weight is m and the plate surface area is S. A reduction of the modal density by a factor of two implies 3 dB less power input and thus 3 dB less noise/vibration.
Weight was not an active output as the weight change between various embossing patterns is ignored in the current analysis scheme. The bulk part of the cab floor weight reduction is made from the removal of the stiffening beams of the reference cab floor.

Modeling guidelines for the seats that are validated up to the 'high' frequencies of the current examination were not available. The seat-floor modes are important for ride comfort and should be included in the model. However, to include the full seat/driver inertia of the low frequency range up to high frequency would probably be very inaccurate. Therefore, a version of the workflow was tested in which chairs are included in the model. It was found that the natural frequencies of the seat-floor modes can be designed to the desired frequencies.

The seats were omitted based on the knowledge that we could not form a useful model of them and that the seat natural frequencies can be controlled with the modal embossing approach. Also, the main objective of the current investigation was to develop a workflow for cab floor embossing optimization, not to design the actual floor.

Whether there in practice is, or is not, a design requirement conflict between seat-floor and NVH designs is thus not known for the examined floor. Nevertheless, in the case a conflict should arise, it would be a problem of the cab floor design, rather than a limitation of the investigated optimization procedure.

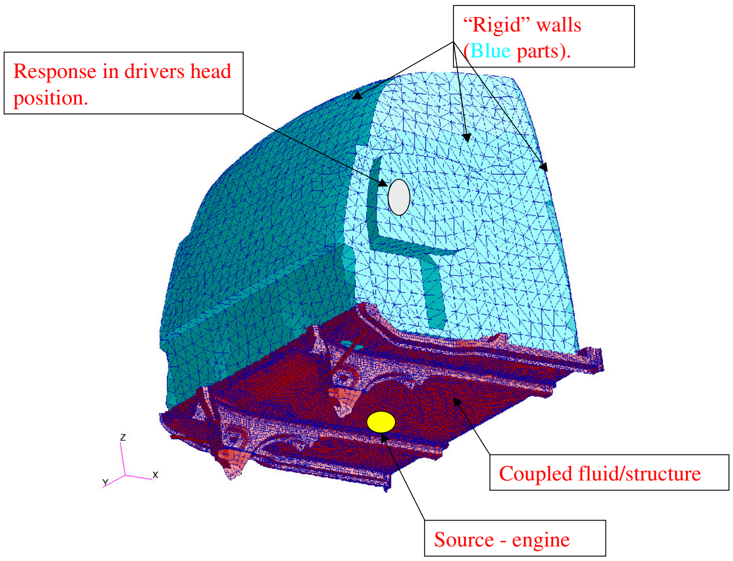

Figure 3. The fully coupled fluid/structure analysis model. ATFs is calculated between points below the floor and the driver and passenger head centre positions. NTFs are calculated between the rear and front support points and the driver and passenger head centre positions.

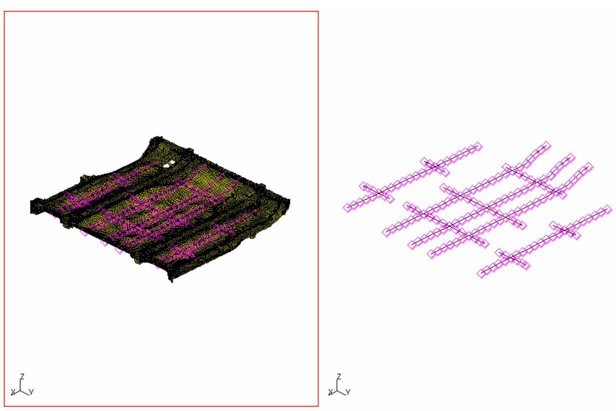

Figure 4. Mode shape tracking by projection of mode shapes onto a simplified mesh. The LHS subfigure shows the mesh from which data is generated. The simplified mesh for mode shape tracking is overlaid on this mesh for comparison. The RHS subfigure shows the simplified mesh that is used for mode shape tracking.

NVH optimization of the cab floor

REFERENCE FLOOR

The old floor design is used as the reference case. The analysis model for the reference case is shown in Figure 5. A fully coupled acoustic analysis revealed the ‘noisy modes’ of the reference floor. The local [1;1] mode of the engine tunnel turned out to be at ~30 Hz and the global [3;1] of the whole floor appears at ~68 Hz.

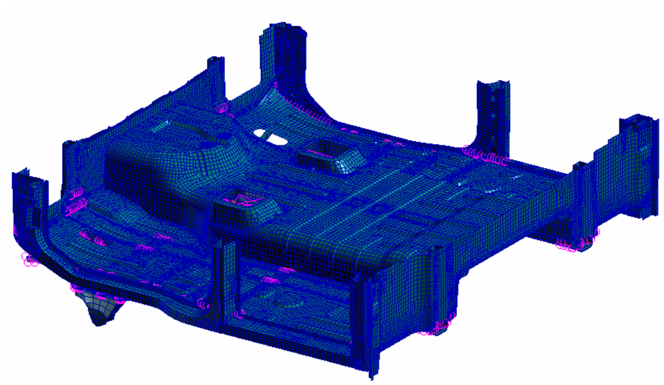

Figure 5. The analysis model for the reference case.

The start out configuration

The start out cab floor is shown in Figure 6. The six noisiest modes of the fully coupled analysis of the flat cab floor are selected for use in the embossing pattern procedure. These modes are: *M1* (1/1 mode); *M3* (3/1 mode); *M8* (5/1 mode); *M9* (1/3 mode); *M11* (1/5 mode); and *M16* (5/3 mode), Figure 7.

Six design variables and the 3 Level Full Factorial (3LFF) Design of Experiments (DoE) procedure necessitates execution of (3^6 =) 729 cases. Each case takes ~3 minutes to analyze, which implies a total execution time of ~36 hours for the 3LFF DoE plan with the computational resources available to us (HP C3600).

The 3LFF DoE test plan is expensive, but sufficient sampling is required when optimizing natural frequencies.

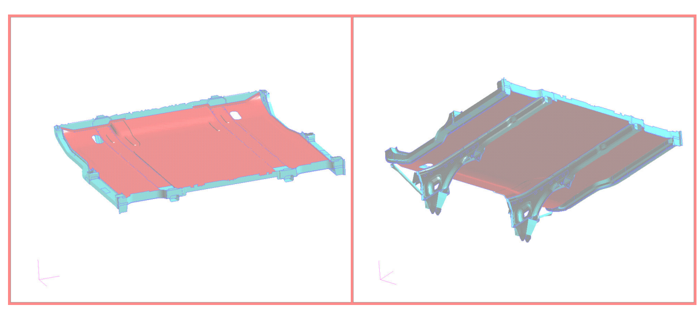

(A) (B)

Figure 6. The start out geometry for the optimization. Mode shapes are imprinted for the plate areas marked in red (darker section) except for the areas that are on top of the main floor beams. A) View from above. B) View from below.

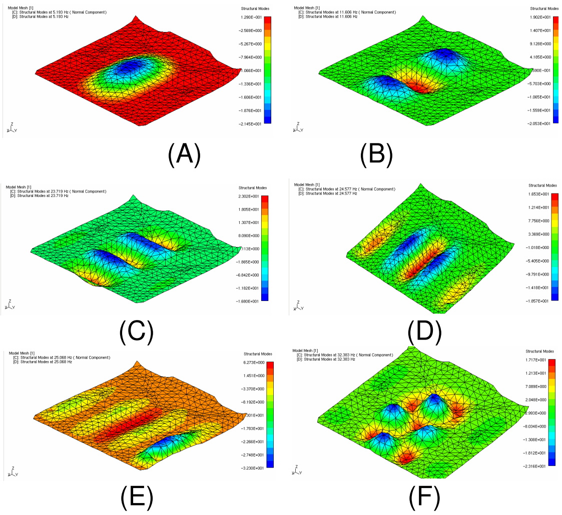

Figure 7. The most ‘noisy’ modes of the flat floor model. A) Mode variable M1. B) Mode variable M3. C) Mode variable M8. D) Mode variable M9. E) Mode variable M11. F) Mode variable M16.

OPTIMIZED FLOOR

Figure 8 shows the optimized floor and the flat floor that was used as start geometry. The optimized floor can be seen to have received a ‘steelpan’ shape (instrument - used in calypso bands).

The ‘noisy’ modes of the optimized floor are located in the frequency bands where they can be tolerated. The [1;1] mode for the intermediate plate section is located at ~40 Hz and the [1;1] modes of the RHS and LHS plate sections are located at ~58 Hz, Figure 9. This design was prompted by the limitations that were created by the dynamic stiffness of the main floor beams, i.e. there is room for further improvement of the floor plate performance if the main floor beams are made stiffer.

Figure 10 show the Acoustic Transfer Functions (ATFs) and Noise Transfer Functions (NTFs) for the reference and the optimized floors. The results show that the optimized floor has a good vibroacoustic performance where noise peaks are located to frequency regions at which engine excitation is swept through quickly during startup. The increase in magnitude for the ATF and NTFs near 83 Hz relates to a cavity resonance that can be counteracted with acoustic treatments.

Note that NTFs shown in Figure 10(a) are the sum or the NTF magnitudes for the x-, y- and z- directions to simplify presentation while keeping track of ‘noise sensitive frequencies’.

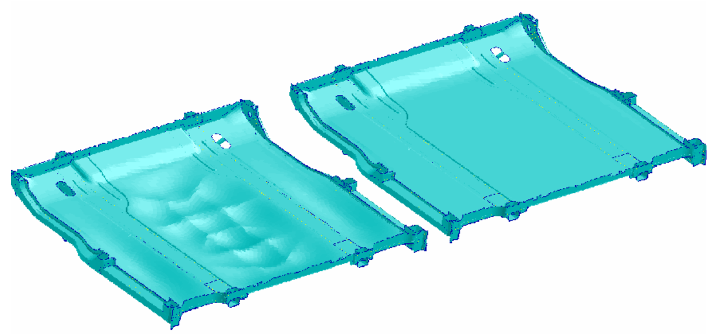

Figure 8. The optimized ‘steelpan’ floor and the flat floor that was used as starting geometry. The maximum imprinting depth is 90 mm.

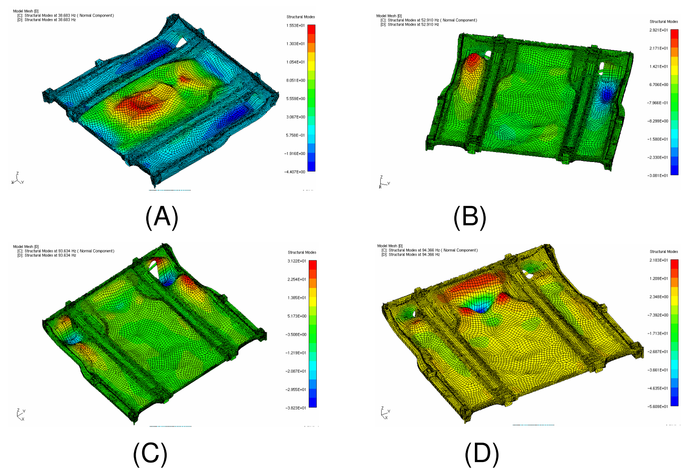

Figure 9. The ‘noisy modes’ of the optimized floor. A) [1;1] mode of the middle floor panel. The main floor beams bend at this frequency, which amplifies sound transmission and the susceptibility to structure-borne noise input. B) [1;1] mode of the LHS and RHS floor panels. C) [3;1] mode of the LHS and RHS floor panels. D) ‘[1,3]’ mode of the middle floor panel.

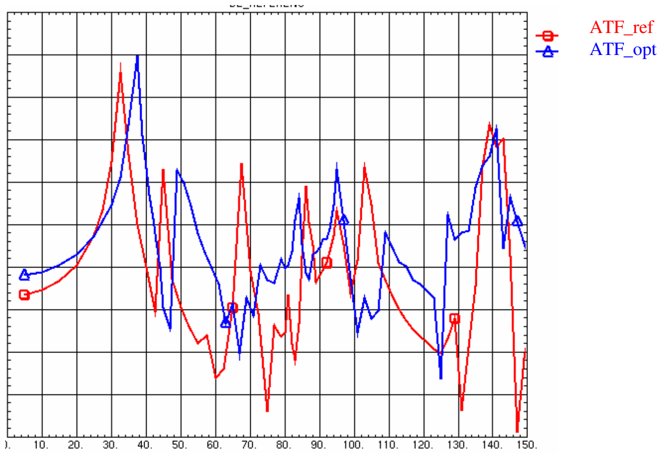

(A)

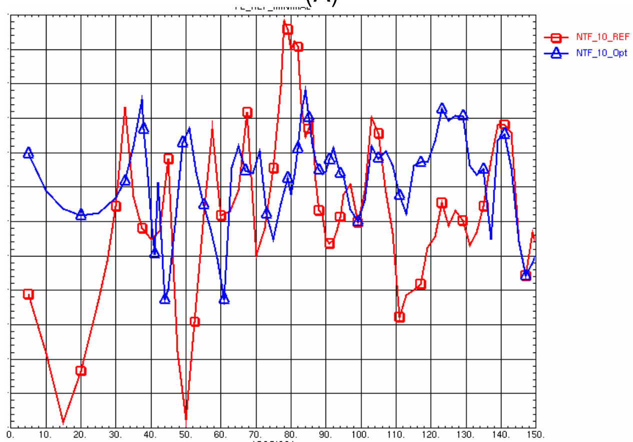

(B)

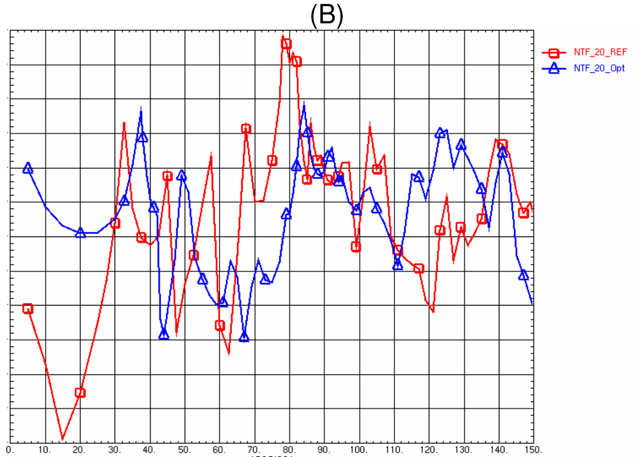

(C)

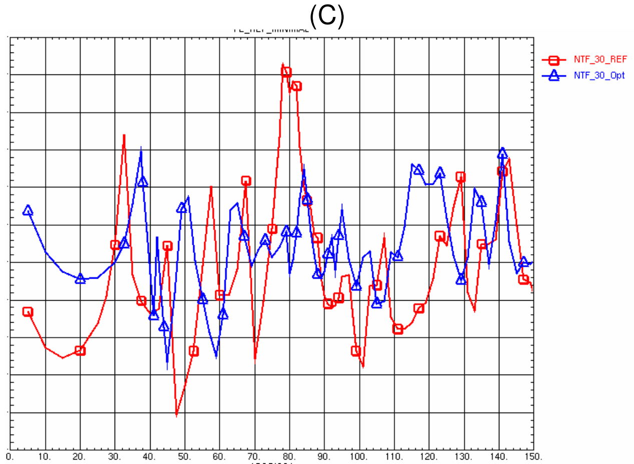

(D)

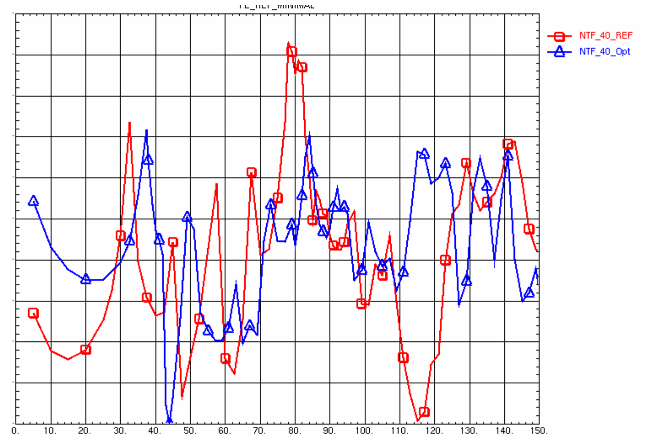

(E)

Figure 10. Computed results for the reference and the optimized floors. Major and minor tick marks on the y-axis represent 5 dB and 1 dB, respectively. A) ATFs for the reference and the optimized floors. B) NTF data for the reference and optimized floors at the LHS front mount position, node 10. C) NTF data for the reference and optimized floors at the RHS front mount position, node 20. D) NTF data for the reference and optimized floors at the LHS rear mount position, node 30. E) NTF data for the reference and optimized floors at the RHS rear mount position, node 40.

MODE COUNT

The first question is whether the effects from embossing ‘stick’ with modes of higher frequency. The modal density is constant for a flat plate, so the mode count becomes a straight line that increase with frequency. However, this statement is only true until the frequency at which the plate sides of the beam break up and act as local plate segments.

The asymptotic trend is that the mode count should become that of the flat plate as soon as any stiffening effects from curvature ‘wear off’. To exemplify, a cylindrical shell has less modes than a flat plate up to its ‘ring frequency’, above which the cylindrical shell behaves just like a flat plate. Of interest is also the fact that the modal density is increased just before the ring frequency.

Figure 11 shows that the starting case of the flat floor leads to a significantly higher number of modes than the reference- and optimized- floors. The number of modes is almost twice as high for this case in comparison with the other floors.

All three floors have a mode count that grows more slowly at frequencies below ~250 Hz. This slower growth is explained by the stiffening effects from curvature and the beams. The mode count grows, as expected, faster at higher frequencies and with a slope that is similar between the floors. It is clear that the slope of the mode count is larger for the flat floor than it is for the optimized floor at all frequencies. Therefore, the effects from curvature can be stated to work up to at least 500 Hz.

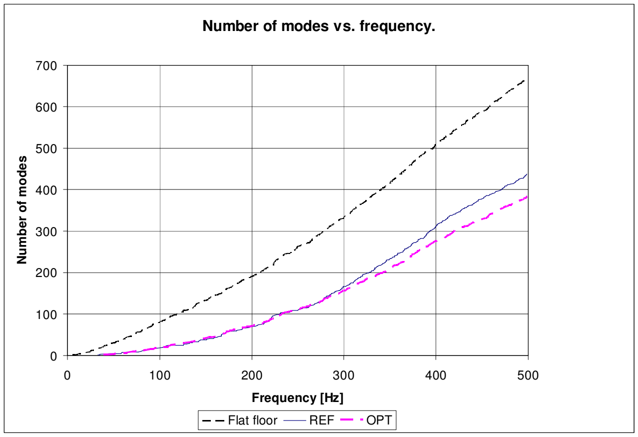

Figure 11. Mode count for the flat- (start out), reference- (REF), and the optimized - (OPT) floors.

CONCLUSIONS

The selection of embossing shape functions from mode shapes was shown to yield sufficient control to guide the natural frequencies of unwanted 'noisy' modes into selected frequency bands. The optimization scheme was deliberately made as simple as possible and mode shape tracking was shown to suffice for the application.

The results show that the optimization enable noise transmission peaks to be shifted into acceptable RPM ranges (of short duration) and that the noise transmission is significantly reduced at idle and for most of the common RPM range (1200 to 1800 RPM).

The optimized floor has significantly reduced weight compared to the reference floor, since the optimized embossing pattern replaces the reinforcing cross beams.

A remaining unwanted peak at ~83 Hz is difficult to remove with embossing as it is affected by an acoustic cab resonance that is best counteracted through acoustic means.

ACKNOWLEDGMENTS

The work reported herein was made for Volvo 3 P - Product Development, as a part of an interior noise research program. A Swedish patent has been applied for the method.

REFERENCES

1. Rebillard E.; Guyader J.L. Hypersensitivity phenomenon on the sound radiated by a population of coupled plates, *15th International Congress on Acoustics Trondheim,* TU26. (1995)
2. Rebillard E.; Guyader J.L. Vibrational Behaviour of Lattices of Plates: Basic behaviour and Hypersensitivity Phenomena, *JSV* **205**(3), p. 337-354. (1997)

CONTACT

The first author can be reached at claes.fredo@ingemansson.se .